Electronic Supplementary Material (ESI) for RSC Advances.

Elucidation of the mechanisms governing the termal diastereomerization of bioactive chiral 1,3,4-thiadiazoline spiro-cyclohexyl derivatives towards their anancomeric stereoisomers.

S. Menta,[a] S. Carradori, [b] G. Siani, [b] D. Secci, [a] L. Mannina, [a] A. P. Sobolev, [c] R. Cirilli *[d] and M. Pierini.*[a]

[a] *Dipartimento di Chimica e Tecnologie del Farmaco, Sapienza Università di Roma, P.le Aldo Moro 5, 00185 Rome, Italy.*

[b] *Department of Pharmacy, "G. D'Annunzio" University of Chieti-Pescara, Via dei Vestini 31, 66100 Chieti, Italy.*

[c] *Laboratorio di Risonanza Magnetica "AnnalauraSegre", Istituto di Metodologie Chimiche CNR Area della Ricerca di Roma, Via Salaria km 29.300, 00015 Monterotondo, Italy.*

[d] *Dipartimento del Farmaco, Istituto Superiore di Sanità, Viale Regina Elena, 299, 00161 Rome, Italy*

E-mails:
marco.pierini@uniroma1.it
roberto.cirilli@iss.it

Table of Contents

.

Scheme S1. General reaction pathway responsible for the *L*→*M* diastereomerization of

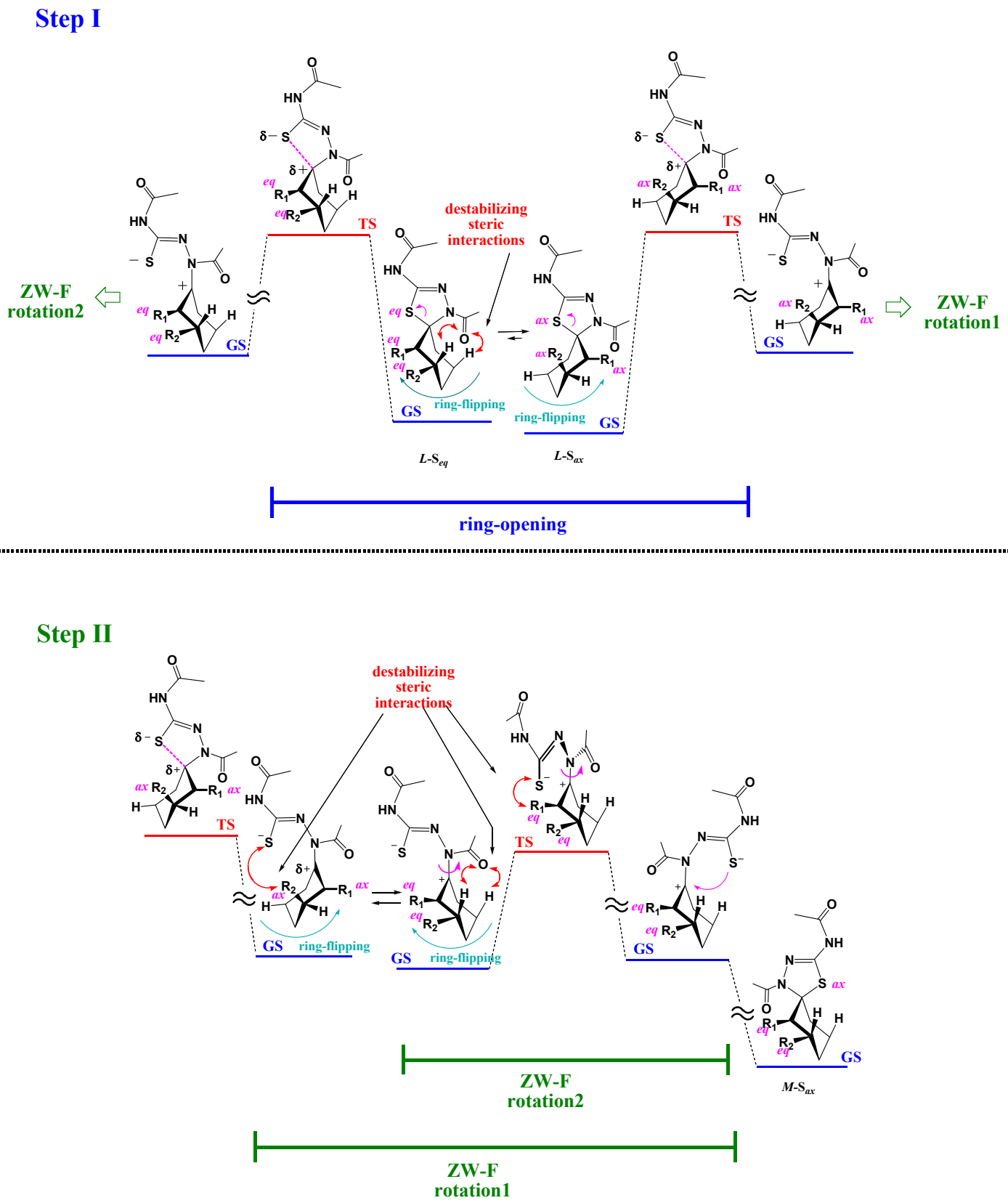

compounds *L*-**1**, *L*-**2** and *L*-**3**.

L-**1**: R_1= CH_3, R_2= H ; *L*-**2**: R_1= *t*-But, R_2= H ; *L*-**3**: R_1= H, R_2= CH_3.

Diastereomerization Mechanism: the adopted molecular modeling procedure.

- ***Evaluation of the ring-opening energy barrier of the thiadiazoline-spiro-cyclohexyl framework (TsC) passing through either the S-C_{spiro} or N-C_{spiro} bond rupture.***

In their first stage, theoretical calculations were focused to shed light about the possible spontaneous opening of the thiadiazoline cycle, only promotable by temperature. In principle, such an opening could engage the sulphur or the nitrogen atom as the leaving group. Although it is well known that, because of its lower basicity, a thiolate anion manifests a greater propensity to act as leaving group with respect to an azanide anion, in the case of the studied compounds this conclusion cannot be assumed as true *a priori*. In fact, the negative charge resulting on the nitrogen atom by rupture of the N-C_{spiro} bond within compounds *L*-**1**, *L*-**2** and *L*-**3** could be quite efficiently delocalized towards both the neighbouring 2-acetamido and 4-acetyl frameworks. For these reasons, the different propensity of the S-C_{spiro} and N-C_{spiro} bonds to undergo rupture has been compared one to each other through the performance of DFT calculations. This molecular modeling analysis was focused on the simplest **TsC** moiety, which is the spiro-framework common to all the considered *L*-**x** compounds (with **x** equal to **1**, **2** or **3**). The comparison was carried out by evaluating the activation barriers $\Delta E^{\#}$ of the spiro ring-opening, calculated by passing through either the S-C_{spiro} or the N-C_{spiro} bond rupture. The analysis was extended to both the two possible conformations of **TsC** (i.e. to the **TsC**-S_{ax} and **TsC**-S_{eq} geometries), optimizing in vacuum the involved transition states. Inspection of the obtained $\Delta E^{\#}$ data (Table S1), highlighted that the rupture of the S-C_{spiro} bond is much more advantageous than that involving the N-C_{spiro} bond, for not less than 32 kcal×mol^{-1}.

Table S1. Absolute and relative DFT energies calculated in vacuum for the N-C_{spiro} and S-C_{spiro} bonds rupture in the S_{ax} and S_{eq} conformations of the **TsC** framework (data computed at the M062X/6-31+G(d)//HF/3-21G level of theory).

Conformation		Energy of TS[a] (a.u.)	$\Delta E^{\#}$ (N-C_{spiro} – S-C_{spiro}) (kcal×mol^{-1})
TsC-S_{ax}	S-C_{spiro} bond rupture	-1141.937327	32.02
	N-C_{spiro} bond rupture	-1141.886302	
TsC-S_{eq}	S-C_{spiro} bond rupture	-1141.944885	36.28
	N-C_{spiro} bond rupture	-1141.887061	
[a] TS: transitions states resulting from the rupture of the S-C_{spiro} or N-C_{spiro} bonds within conformations S_{ax} and S_{eq} of model **TsC**			

- ***Evaluation of the ring-opening energy barrier in Step I of the general reaction pathway resumed in Scheme 1 requiring the S-C_{spiro} bond rupture.***

On the base of the above key information, the DFT optimization of the transition states leading to the S-C_{spiro} bond rupture (corresponding to Step I of the hypothesized reaction pathway reported in Scheme S1) was performed in chloroform, as common solvent of reference, on the **TsC** framework, and afterwards also on the structures of *L*-**1**, *L*-**2** and *L*-**3**. For each species we took into consideration both the conformations of type S_{ax} and S_{eq}. The computed absolute energy stabilities have then been collected in Table S2. About these data, it is useful to stress that the energy stabilities corresponding to the related geometries at the ground state were already computed in our previous study, cited in reference 36.

Table S2. Absolute DFT energy stabilities of ground and transition states involved in Step I and Step II of the considered reaction pathways of compounds *L*-**1**, *L*-**2** and *L*-**3** and **TsC** framework, computed at the M062X/6-31+G(d)//B3LYP/6-31G(d) level of theory in some different solvents.

Compound	*Config.*	*Conf.*	*Stage of ring-opening (Step I)*		*Stage of ZW-F-rotation (Step II)*	
			GS [a] (μ; V)	TS (μ; V)	GS (μ; V)	TS (μ; V)
Calculations performed in chloroform according to the SM8 solvation model						
1	(5*R**, 6*S**)	alkyl$_{eq}$, S$_{ax}$	-1181.30784 (4.99; 267.59)	-	-	-
	(5*R**, 6*S**)	alkyl$_{ax}$, S$_{eq}$	-1181.293355 (5.42; 267.02)	-	-	-
	(5*R**, 6*R**)	alkyl$_{ax}$, S$_{ax}$	-1181.301539 (5.27; 267.07)	-1181.258325 (6.80; 271.92)	-1181.25923	-1181.21991
	(5*R**, 6*R**)	alkyl$_{eq}$, S$_{eq}$	-1181.298624 (5.35; 267.35)	-1181.25133 (8.84; 272.84)	-1181.25212	-1181.21483
2	(5*R**, 6*R**)	alkyl$_{eq}$, S$_{ax}$	-1299.181704 (5.21; 320.71)	-	-	-
	(5*R**, 6*R**)	alkyl$_{ax}$, S$_{eq}$	-1299.160522 (5.53; 320.11)	-	-	-
	(5*R**, 6*S**)	alkyl$_{ax}$, S$_{ax}$	-1299.170536 (5.54; 320.50)	-1299.134981 (6.12; 325.11)	-1299.13905	-1299.09625
	(5*R**, 6*S**)	alkyl$_{eq}$, S$_{eq}$	-1299.170152 (5.44; 320.37)	-1299.126011 (6.33; 324.72)	-1299.12745 (12.66; 326.05)	-1299.08561 (9.46; 327.23)
3	(5*R**, 7*R**)	alkyl$_{eq}$, S$_{ax}$	-1181.307748 (5.16; 267.52)	-	-	-
	(5*R**, 7*R**)	alkyl$_{ax}$, S$_{eq}$	-1181.296056 (5.74; 267.21)	-	-	-
	(5*R**, 7*S**)	alkyl$_{ax}$, S$_{ax}$	-1181.302628 (4.98; 267.47)	-1181.256503 (6.09; 271.66)	-	-
	(5*R**, 7*S**)	alkyl$_{eq}$, S$_{eq}$	-1181.299622 (5.55; 267.4)	-1181.2612474 (7.63; 272.12)	-	-
TsC	-	S$_{ax}$	-1142.011244 (5.07; 249.38)	-1141.964556 (6.66; 254.02)	-1141.96613	-1141.92750
	-	S$_{eq}$	-1142.002881 (5.45; 249.28)	-1141.965033 (7.08; 253.73)	-1141.96619	-1141.92936
Calculations performed in ethyl acetate according to the SM8 solvation model						
2	(5*R**, 6*S**)	alkyl$_{eq}$, S$_{eq}$	-	-	-1299.12743 (12.39; 325.71)	-1299.08522 (9.63; 327.15)
Calculations performed in 2-propanol according to the SM8 solvation model						
2	(5*R**, 6*S**)	alkyl$_{eq}$, S$_{eq}$	-	-	-1299.12991 (14.21; 326.23)	-1299.08529 (11.38; 327.47)
Calculations performed in water according to the SM8 solvation model						
1	(5*R**, 6*R**)	alkyl$_{ax}$, S$_{ax}$	-1181.29542	-1181.25299		
	(5*R**, 6*R**)	alkyl$_{eq}$, S$_{eq}$	-1181.29181	-1181.24784		
2	(5*R**, 6*S**)	alkyl$_{ax}$, S$_{ax}$			-1299.13199	-1299.09006
	(5*R**, 6*S**)	alkyl$_{eq}$, S$_{eq}$			-1299.12299	-1299.07660
3	(5*R**, 7*S**)	alkyl$_{ax}$, S$_{ax}$	-1181.29658	-1181.25131		
	(5*R**, 7*S**)	alkyl$_{eq}$, S$_{eq}$	-1181.29337	-1181.25686		

Config.: relative configuration of the structure; *Conform.*: axial or equatorial disposition assumed by the alkyl group and sulphur atom within each conformation; *Step I* and *Step II*: stages of ring-opening and ZW-F-rotation of the *L*→*M* diastereomerization processes; μ: dipole moment; V: molecular volume.

[a] Energy values reported in reference 36 of main text.

Evaluation of the ZW-F-rotation energy barrier in Step II of the general reaction pathway of Scheme 1.

Starting from the optimized S_{ax} conformations in chloroform of the species *L*-**1**-ZW-S_{ax}, *L*-**2**-ZW-S_{ax} and **TsC**-ZW-S_{ax}, which come from the ring-opening stage in Step I, and are therefore endowed with zwitterionic structure, it was computed the energy profile resulting from the progressive change of the dihedral angle related to the torsional N–N–C_{spiro}–CH_2 defined in Figure S1. Next, the same procedure was also repeated by starting from the ring-flipped zwitterionic S_{eq} conformers, symbolized hereafter as *L*-**x**-ZW-S_{eq}, whose generation from the S_{ax} isomers is obviously expected to take place very fast, and therefore through a stereochemical event unable to influence the extent of the isomerization barriers. In this latter S_{eq} species, the sulphur atom appears slightly raised with respect to the alkyl substituent, and so more prone to allow faster rotation. From these energy profiles we could be assessed the related ZW-F-rotation energy barriers $\Delta E^{\#}_{L\rightarrow M}$, corresponding to the slow-stage of Step II of the proposed reaction pathway. For the species *L*-**2**-ZW-S_{eq} the $\Delta E^{\#}_{L\rightarrow M}$ barrier was also evaluated in ethyl acetate and 2-propanol by re-optimizing in these solvents the GS and TS geometries already obtained in chloroform. A graphical representative example of application of this type of procedure is reported in Figure S1 for the particular case of *L*-**2**-ZW-S_{eq}. All the findings coming from these calculations have been collected in Table S2.

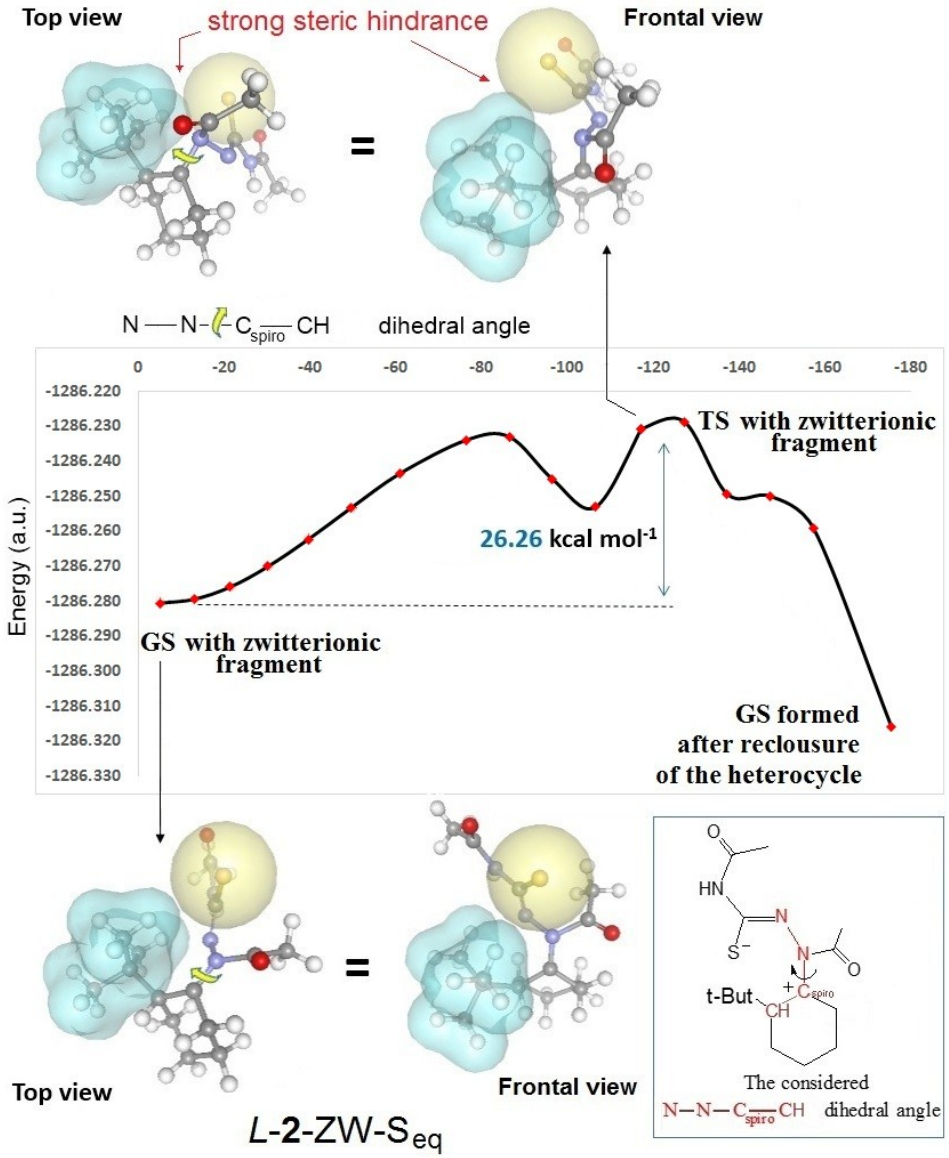

Figure S1. ZW-F-rotation pathway computed at the HF3-21G level of theory in chloroform for *L*-**2**-ZW-S_{eq}. The obtained GS and TS geometries were afterwards optimized in chloroform at the B3LYP/6-31G(d) level of theory and then submitted to single point energy calculation, always in the same solvent, through the M062X/6-31+G(d) method.

The assessed activation energies governing Step I and Step II of the general reaction-pathway reported in Scheme 1 involving the TsC framework.

In the simplified case of the **TsC** framework, DFT calculations suggested that the barrier involved in Step I of the general reaction pathway reported in Scheme 1 (that necessarily concerns the anancomeric conformer **TsC**-S_{ax}) is characterized by the quite high activation energy of 29.3 kcal×mol^{-1}. On the contrary, the barriers computed for Step II, arising by rotation of the zwitterionic fragments generated in **TsC**-ZW-S_{ax} and **TsC**-ZW-S_{eq} through Step I, are much lower. In fact, the one coming from the **TsC**-ZW-S_{ax} conformer achieved the value of 24.2 kcal×mol^{-1}, while the other a value of 23.1 kcal×mol^{-1}. In Scheme S2 we resumed the most energetically convenient stages involved in the ring-opening and ZW-F rotation processes concerning **TsC**, useful for comparison purposes with the species *L*-**1** and *L*-**2**.

Scheme S2. Activation energies for the ring-opening and ZW-F-rotation involving the **TsC** framework, computed in chloroform at the M062X/6-31+G(d)//B3LYP/6-31G(d) level of theory.

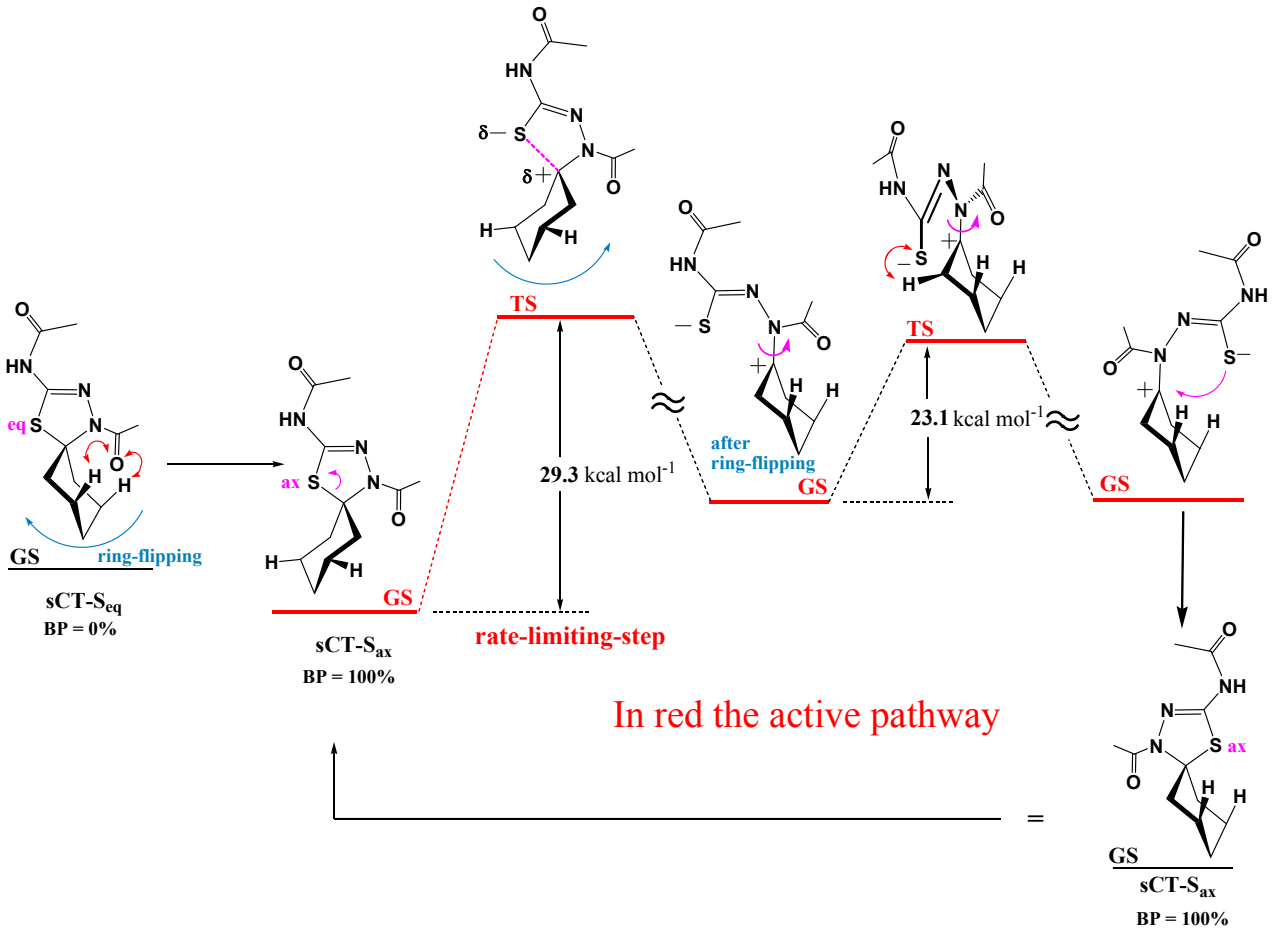

- ***Diastereomerization mechanism involving compound L-1.***

For compound *L*-**1** calculations assessed a difference of 2.4 kcal×mol^{-1} between the quite high $\Delta E^{\#}_{L\rightarrow M}$ values of the ring-opening barriers computed starting from the couple of conformations *L*-**1**-S_{ax} ($\Delta E^{\#}_{L\rightarrow M}$=27.1 kcal×mol^{-1}) and *L*-**1**-S_{eq} ($\Delta E^{\#}_{L\rightarrow M}$=29.7 kcal×mol^{-1}). Thus, about the individuation of the most energetically convenient pathway governing kinetically the Step I of the *L*-**1**→*M*-**1** process, it is predicted that this must involve the more stable geometry *L*-**1**-S_{ax}. Instead, the energy barriers estimated for the ZW-F rotation in Step II of the same diastereomerization were characterized by much lower values: 24.7 kcal×mol^{-1} from the *L*-**1**-ZW-S_{ax} conformer, while 23.4 kcal×mol^{-1} from its ring-flipped *L*-**1**-ZW-S_{eq} counterpart. Thus, according to the principle of the bottleneck applied to the case of consecutive and irreversible two-step reactions (as, in fact, occurs for all the here considered *L*-**x**→*M*-**x** isomerizations, because of the much greater stability that all the anancomeric species *M*-**x**-S_{ax} show, compared to their diastereomers *L*-**x**, which leads the alkyl groups to rapidly lose the axial disposition in favour of the equatorial one, and with it, also the geometric requirement for a fast back-reclosure of the cycle), it may be reasonably concluded that for the *L*-**1**→*M*-**1** process Step I is the one governing the energy barrier of the isomerization. The complete reaction pathway suggested for the *L*-**1**→*M*-**1** process by the just quoted energy data, is schematized in Scheme 3.

Scheme S3. Activation energies involved in the *L*-**1**→*M*-**1** diastereomerization process, computed in chloroform at the M062X/6-31+G(d)//B3LYP/6-31G(d) level of theory.

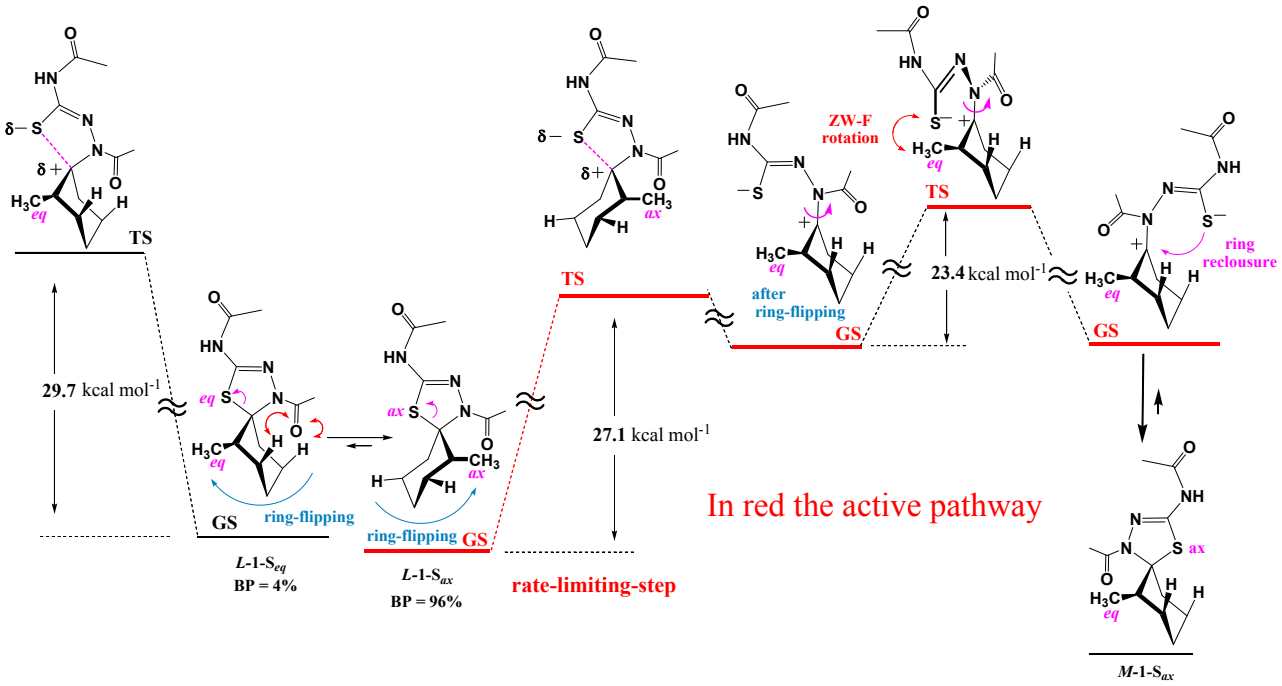

- ***Diastereomerization mechanism involving compound L-3.***

A bit different from the case discussed for the species *L*-**1** is the situation found for compound *L*-**3**. In fact, starting from the most stable conformation of this latter species (that is to say the *L*-**3**-S_{ax} geometry), the computed $\Delta E^{\#}_{L\rightarrow M}$ barrier of ring-opening amounts to 28.9 kcal×mol^{-1} while, instead, to only 24.1 kcal×mol^{-1} if the ring-opening is considered starting from the 1.89 kcal×mol^{-1} (Table S1) less stable ring-flipped *L*-**3**-S_{eq} counterpart. Since the assessed Boltzmann Populations of these two conformational ground states are 96% and 4%, respectively, it is reasonable to admit that the active kinetic pathway governing Step I of the *L*-**3**→*M*-**3** diastereomerization must requires a fast initial conformational change, from the more abundant *L*-**3**-S_{ax} geometry to the less populated *L*-**3**-S_{eq} isomer. Thus, thanks to this forced, but fast, interconversion, the species *L*-**3** will be able to undergo

ring-opening through an activation energy reduced of as much as 4.9 kcal×mol^{-1}. Nevertheless, for a reliable estimation of the ring-opening barrier, both the activation energy requested by the S-C_{spiro} bond rupture in *L*-**3**-S_{eq} and the brake exercised by the need of the *L*-**3**-S_{ax} →*L*-**3**-S_{eq} conversion have to be suitably taken into account at the same time. The approach pursued to achieve this goal will be discussed in the next sub-section titled "*Simulation of the time-dependent decay of L-**3***".
Instead, about the estimation of the couple of possible energy barriers connected to Step II of the *L*-**3**→*M*-**3** diastereomerization, these were not explicitly computed. Indeed, it was expected that, in the present case, the activation energies relevant to the ZW-F rotation involving the *L*-**3**-ZW-S_{ax} and *L*-**3**-ZW-S_{eq} conformers could not be greater than those already calculated for *L*-**1**-ZW-S_{ax} and *L*-**1**-ZW-S_{eq}, species in which the methyl group, being much closer to the C_{spiro} reaction centre, is certainly bearer of greater intramolecular hindrance. For these reasons, in the reaction pathway of the *L*-**3**→*M*-**3** process resumed in Scheme S4, the $\Delta E^{\#}_{L\rightarrow M}$ barrier governing the slow-stage of Step II was generically given as internal to the range of 23.1÷23.4 kcal×mol^{-1}. The extremal values of such a range are, in fact, the lower barriers estimated for the ZW-F rotation in the zwitterionic forms generated by **TsC** and *L*-**1**, respectively.

*Simulation of the time-dependent decay of L-**3***
Resorting to all the above calculated data (i.e. the $\Delta E^{\#}_{L\rightarrow M}$ barrier of 24.1 kcal×mol^{-1}, from which it was derived the related $k_{L\rightarrow M}$ kinetic constant at 55 °C, and the relative abundances 96% and 4% of the species *L*-**3**-S_{ax} and *L*-**3**-S_{eq}), the time-dependent decay of *L*-**3** was successful simulated through the suitable computer program Achem. This is a software specifically designed for modeling complex chemical reaction systems (for more information about it see reference 37 reported in the paper). The used input file, with annexed legend and relevant description, is attached at the end of this section). From the simulation it was derived the value of the diastereomerization constant $k_{L\rightarrow M}$ (2.1×10^{-3} min^{-1}) and, through it, also the related activation barrier $\Delta E^{\#}_{L\rightarrow M}$ at 55°C, to be compared with the relevant experimental one (calculated datum: $\Delta E^{\#}_{L\rightarrow M}$ = 26.0 kcal×mol^{-1}; experimental datum: $\Delta G^{\#}_{L\rightarrow M}$ = 25.5 kcal×mol^{-1}, Figure S2).

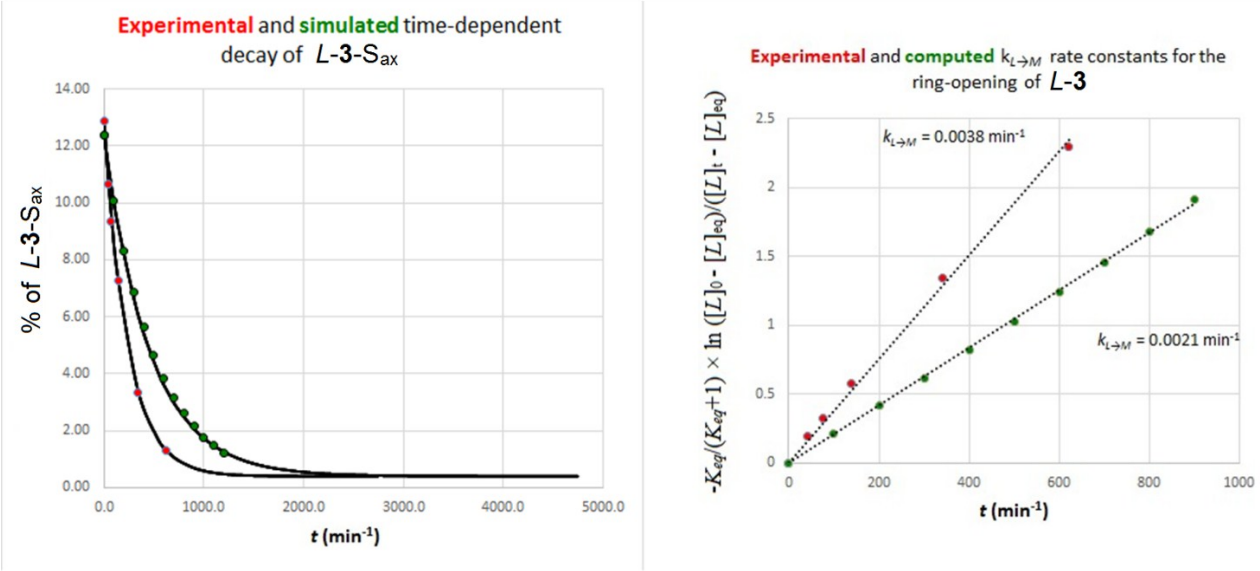

Figure S2. Simulation of the time-dependent decay of *L*-**3** in chloroform at 55 °C and relevant determination of the associated forward $k_{L\rightarrow M}$ rate constant. In red and green are reported the experimental and simulated data, respectively.

Scheme S4. Activation energies involved in the *L*-**3**→*M*-**3** diastereomerization process, computed in chloroform at the M062X/6-31+G(d)//B3LYP/6-31G(d) level of theory.

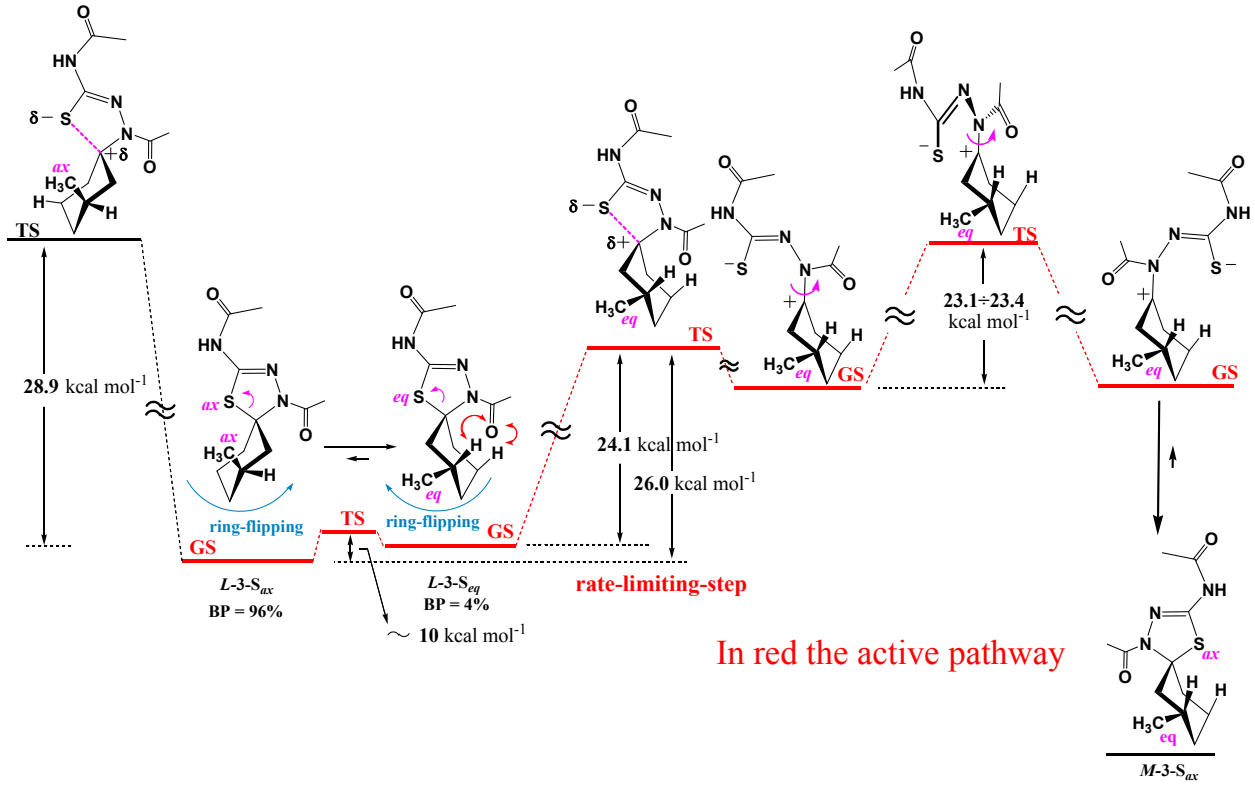

Input file used in Achem program to simulate the time-dependent decay of compound L-**3**.

Legend: a= species *L*-**3**-S_{ax}; b= species *L*-**3**-S_{eq}; c= species *L*-**3**-ZW-S_{eq}; a=b and b=a symbolize the forward $k_{ax\rightarrow eq}$ and backward $k_{eq\rightarrow ax}$ rate constants in the input file.
The rate constants $k_{ax\rightarrow eq}$ and $k_{eq\rightarrow ax}$ involved into the *L*-**3**-S_{ax}⇆*L*-**3**-S_{eq} equilibrium of ring-flipping were computed at 55 °C starting from activation energies that differed one to each other for 1.89 kcal×mol^{-1} (i.e. the difference in energy stability assessed by calculation between *L*-**3**-S_{ax} and *L*-**3**-S_{eq}). The lower of these two ($\Delta E^{\#}_{ax\rightarrow eq}$) was arbitrarily imposed to 10 kcal×mol^{-1}, in order to reflect a fast equilibrium and to be reasonable close to the true data. The values assigned to the rate constants symbolized as a = c and b = c were instead calculated at 55 °C from the assessed $\Delta E^{\#}$ ring-opening values of 28.9 and 24.1 kcal×mol^{-1}, respectively. It is important to stress that the absolute value chosen for $\Delta E^{\#}_{ax\rightarrow eq}$ (which is of the order of magnitude of a classical cyclohexane-ring flipping) is irrelevant to the result, provided that it is much lower than that concerning the ring-opening.

;input file
compound *L*-3
1101
1, a = b, 4.87E6
2, b = a, 8.84E7
3, a = c, 2.32E-5
4, b = c, 3.65E-2
END
a, 96.0
b, 4.0
END
0.001
0.0,
100.0,
:
2200.0,
2300.0

*The differential role played by the methyl group in compounds L-**1** and L-**3**.*

Interesting information about the differential effect exercised by the methyl group in the constitutional isomers *L*-**1** and *L*-**3** has been obtained by comparing both the kinetic and thermodynamic behavior assessed for these latter species with that estimated for **TsC**. As expected, because of the absence in **TsC** of a substituting alkyl group able to affect by steric hindrance the stability of the relevant both ground and transition states, for the anancomeric geometry **TsC**-S_{ax} (therefore endowed with BP=100%) the S-C_{spiro} bond rupture was assessed to require a $\Delta E^{\#}$ barrier greater than those found for *L*-**1** and *L*-**3**. In fact, for the ring-opening in **TsC**-S_{ax} the estimated barrier was 29.3 kcal×mol^{-1}, while for the same S-C_{spiro} bond rupture in *L*-**1** and *L*-**3** the barriers were 27.1 kcal×mol^{-1} and 28.9 kcal×mol^{-1}, respectively. Nevertheless, in the whole, the predicted kinetic trend of **TsC** was coherently found not too far from that of *L*-**3**, according with the relatively long distance that the methyl moiety displays in this latter species from the reaction-center (i.e. the C_{spiro} atom). In fact, the differential perturbing effect exercised by the methyl group on the $\Delta E^{\#}_{L\rightarrow M}$ barrier (easily observable when passing from **TsC** to *L*-**3** or to *L*-**1**) can be resumed in two simple points (see data in Table S2):

i) with respect to what happens for the ring-opening of **TsC** starting from its S_{ax} conformation, the equivalent $\Delta E^{\#}_{L\rightarrow M}$ barrier decreases of only 0.4 kcal×mol^{-1} in the case of compound *L*-**3**, while of as many as 2.2 kcal×mol^{-1} in the case of compound *L*-**1;**

ii) with respect to what happens for the ring-opening of **TsC** starting from its S_{eq} conformation, the equivalent $\Delta E^{\#}_{L\rightarrow M}$ barrier increases of only 0.3 kcal×mol^{-1} in the case of compound *L*-**3**, while of as many as 5.9 kcal×mol^{-1} in the case of compound *L*-**1**.

Instead, in spite of the quite similar kinetic trend, the very important difference observable between compound *L*-**3** and model **TsC** has thermodynamic origin. This is because in *L*-**3**-S_{ax} the presence of the methyl group breaks the anancomeric character possessed by its **TsC**-S_{ax} framework when devoid of any alkyl substituent (which, is useful to remind, is more stable of its ring-flipped counterpart **TsC**-S_{eq} by 5.24 kcal×mol^{-1}). Such an effect reduces the difference of thermodynamic stability existing between the *L*-**3**-S_{ax} and *L*-**3**-S_{eq} conformations to only 1.89 kcal×mol^{-1}, making possible the existence of the *L*-**3**-S_{eq} structure in a BP of about 4%, and therefore, also its possible involvement into the considered diastereomerization process, as already stressed above.

- ***Diastereomerization mechanism for compound 2.***

With respect to the diastereomerizations suffered by *L*-**1** and *L*-**3**, the case of compound *L*-**2** was found much different. For it, indeed, calculations revealed that, between the two possible less stable conformational stereomers *L*-**2**-S_{ax} and *L*-**2**-S_{eq}, the most convenient ring-opening pathway under an energetic point of view should involve the most abundant one (the one displaying the S_{ax} conformation). For this latter species, in fact, the required energy barrier to be overcome is of only 22.3 kcal×mol^{-1}, while starting from the other S_{eq} conformer the found $\Delta E^{\#}_{L\rightarrow M}$ value is instead of 27.7 kcal×mol^{-1}. The reasons for the existence of such a macroscopic difference, when compared to the cases of compounds *L*-**1** and *L*-**3**, is attributable to the strong structural destabilization that in *L*-**2** the *t*-butyl exerts on the geometry of the ground state *L*-**2**-S_{ax} (in which it is in axial position), much greater of that suffered by its related transition state. This is also reflected on the minimal increase of energy (0.2 kcal×mol^{-1}) found by calculation moving from the *L*-**2**-S_{ax} to the *L*-**2**-S_{eq} conformer, against the much greater differences of 1.83 and 1.89 kcal×mol^{-1} found by comparing the analogue type of conformers in *L*-**1** and *L*-**3**, respectively. Thus, the estimated activation energy of 22.3 kcal×mol^{-1} for the S-C_{spiro} bond breaking does not match the experimental datum relevant to the *L*-**2**→*M*-**2** process that, in chloroform, amounts to 25.5 kcal×mol^{-1}. However, the visual inspection of the model of the zwitterionic structure *L*-**2**-ZW-S_{ax}, formed by ring-opening in Step I,

clearly suggests that, in this case, the subsequent rotation of the thiadiazo-arm, needed to enable the inversion of configuration of the C_{spiro} carbon, although promoted in synergic fashion by both the greater stability possessed by the generated anancomeric product *M*-**2**-S_{ax} and the fast and irreversible loss of the axial arrangment suffered by the *t*-butyl substituent, should be made particularly difficult by the considerable steric hindrance associated to the *t*-butyl group. An equivalent steric hindrance, instead, is not inferable for compounds *L*-**1** and *L*-**3**. Accordingly, the assessed energy barriers relevant to the ZW-F rotation (Figure S1) resulted in this case much greater than that due to the spiro ring-opening, achieving the values of 26.86 kcal×mol^{-1}, starting from the *L*-**2**-ZW-S_{ax} conformer, and 26.26 kcal×mol^{-1}, from the ring-flipped *L*-**2**-ZW-S_{eq} counterpart. In the whole, then, it may be stated that the rate-limiting stage characterizing the kinetic of the *L*-**2**→*M*-**2** diastereomerization must not be identified with the ring-opening suffered by the compound in Step I, but, instead, with the ZW-F-rotation that occurs on the zwitterionic species in Step II. Also in this case, therefore, again in respect of the principle of the bottleneck applied to the case of consecutive and irreversible two-step reactions, the existing agreement between predicted and experimental values of the energy barrier governing the *L*-**2**→*M*-**2** diastereomerization in chloroform sounds very good, being of only 0.7 kcal×mol^{-1} the found energy discrepancy. In Scheme S5 they were resumed all the elemental steps constituting the overall reaction pathway of the *L*-**2**→*M*-**2** process, inclusive of the computed barriers.

Scheme S5. Activation energies involved in the *L*-**2**→*M*-**2** diastereomerization process, computed in chloroform at the M062X/6-31+G(d)//B3LYP/6-31G(d) level of theory.

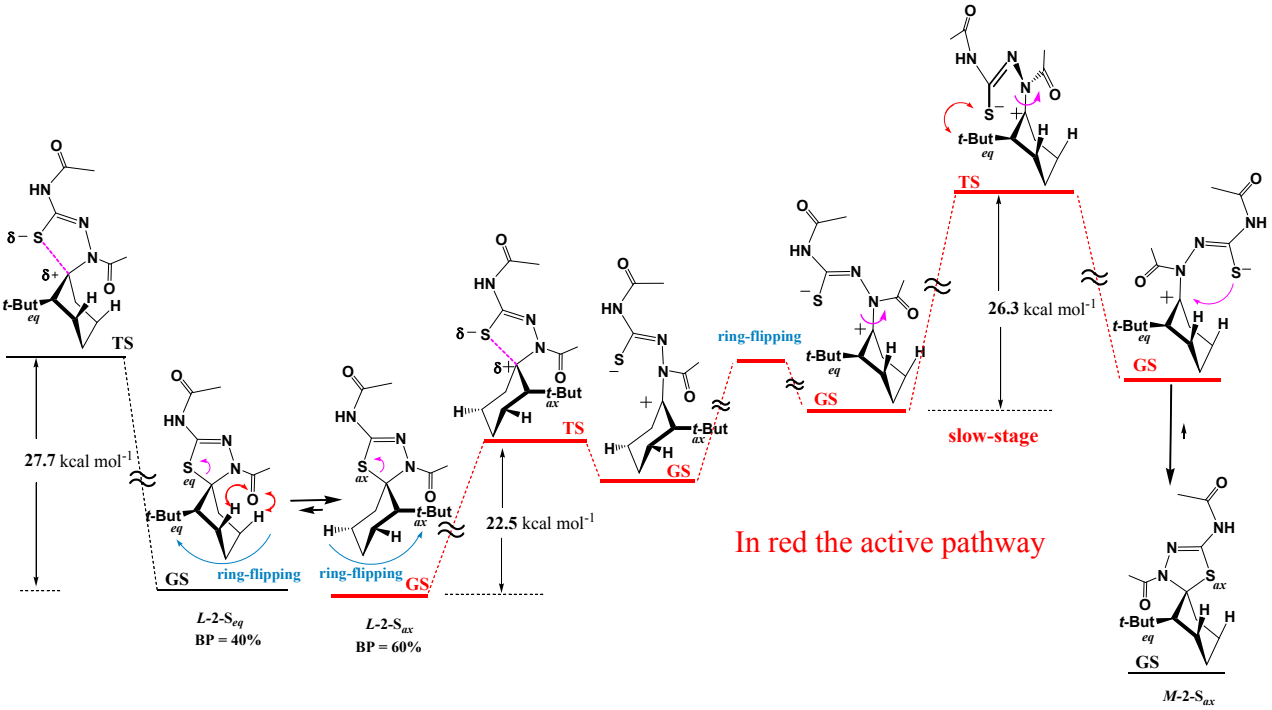

Eventually, as already anticipated, in order to take into account the effect played on the *L*-**2**→*M*-**2** isomerization by a change of solvent, only for this latter compound the ZW-F-rotation barrier $\Delta E^{\#}_{L\rightarrow M}$ was also recomputed in ethyl acetate and 2-propanol, the only other media, beside the chloroform, available in the SM8 solvation model implemented in Spartan. Accordingly, the geometries of the ground and transition states related to the above *L*-**2**-ZW-S_{eq} structure (that originally were modeled and optimized in chloroform), were submitted to new optimizations in both ethyl acetate and 2-propanol. From them, the $\Delta E^{\#EA}_{L\rightarrow M}$ (26.49 kcal×mol^{-1}) and $\Delta E^{\#IPA}_{L\rightarrow M}$ (28.00 kcal×mol^{-1}) energy barriers were computed and, again, found in very good agreement with the equivalent experimental ones, by only -0.35 and +0.22 kcal×mol^{-1}, respectively.

Table S3**. Results of the LSER analyses carried out on compounds* L-1,*** L-***2*** *and* L-***3***

Entry	Compound	Descriptors (t_i)		index-T	index-F	R^2
1	**1**	π^* (3.05)	–	2.28	0.09	0.8230
2		ε (0.91)	–	2.28	0.46	0.2922
3		δ_H^2 (0.44)	–	2.28	0.70	0.0881
4		π^* (34.13)	δ_H^2 (15.01)	4.17	0.03	0.9992
5		ε (12.47)	δ_H^2 (10.97)	4.17	0.08	0.9942
6	**2**	π^* (5.49)	–	2.28	0.03	0.9378
7		ε (0.46)	–	2.28	0.69	0.0942
8		δ_H^2 (0.07)	–	2.28	0.95	0.0027
9		π^* (5.73)	δ_H^2 (1.06)	4.17	0.17	0.9705
10		ε (3.45)	δ_H^2 (3.28)	4.17	0.28	0.9228
11	**3**	π^* (4.28)	–	2.28	0.05	0.9017
12		ε (0.68)	–	2.28	0.57	0.1861
13		δ_H^2 (0.26)	–	2.28	0.82	0.0320
14		π^* (14.82)	δ_H^2 (4.63)	4.17	0.07	0.9956
15		ε (5.60)	δ_H^2 (5.12)	4.17	0.17	0.9701

Cartesian Coordinates of TS-(5*R**, 6*R**)-**1-S$_{ax}$** in chloroform, imaginary frequency: - 51.706 cm^{-1}

37
M0001 0.000000
S 0.8686 0.7459 1.4651
C 1.4176 -0.0917 0.0718
N 0.7030 -0.8779 -0.7422
N -0.5834 -1.1374 -0.2708
C -0.8287 -2.5328 0.0799
C 0.3976 -3.3776 0.2667
O -1.9643 -2.9481 0.1604
N 2.7323 -0.0405 -0.3879
C 3.8377 0.7073 0.0029
C 5.0495 0.4361 -0.8691
O 3.8523 1.4953 0.9350
H 1.0712 -2.9378 1.0087
H 0.9569 -3.4571 -0.6700
H 0.0731 -4.3671 0.5914
H 5.9014 0.9912 -0.4755
H 4.8627 0.7528 -1.9020
H 5.2924 -0.6322 -0.8872
H 2.8763 -0.6432 -1.1979
C -1.4802 -0.1568 -0.1375
C -1.9937 2.3326 -0.4134
C -3.2768 0.9621 1.2492
C -3.3657 2.0932 0.2244
C -2.7639 -0.3507 0.6228
C -1.3775 1.0625 -1.0337
H -1.3019 2.7124 0.3471
H -2.6053 1.2529 2.0668
H -4.1118 1.8430 -0.5419
H -2.0567 3.0967 -1.1969
H -4.2564 0.7591 1.6953
H -3.7140 3.0143 0.7061
H -2.6564 -1.1232 1.3829
H -0.3326 1.2575 -1.2669
H -3.5147 -0.7335 -0.0837
C -2.0725 0.6708 -2.3700
H -1.5945 -0.2019 -2.8259
H -1.9784 1.5091 -3.0685
H -3.1371 0.4549 -2.2449

Cartesian Coordinates of TS-(5*R**, 6*R**)-**1-S$_{eq}$** in chloroform, imaginary frequency: - 19.110 cm^{-1}

37
M0001 0.000000
S 1.5055 -0.2645 1.8142
C 1.5475 -0.1540 0.1105
N 0.5435 -0.2956 -0.7679
N -0.6801 -0.6683 -0.2277
C -0.9409 -2.1178 -0.5712
C -0.1346 -3.1201 0.1893
O -1.7343 -2.3437 -1.4473
N 2.7085 0.1388 -0.6168
C 4.0089 0.4549 -0.2388
C 4.8925 0.7601 -1.4357
O 4.4181 0.4970 0.9100
H 0.9355 -2.9624 0.0306
H -0.4191 -4.1182 -0.1472
H -0.3110 -3.0087 1.2635
H 5.9109 0.9342 -1.0867
H 4.5362 1.6550 -1.9592
H 4.8933 -0.0681 -2.1535
H 2.5360 0.1563 -1.6210
C -1.6086 0.0985 0.2674
C -4.1028 -0.0953 -0.0278
C -2.8648 2.0420 -0.5661

C -4.1855 1.4315 -0.0889
C -1.6260 1.6130 0.2914
C -2.8717 -0.5352 0.7941
H -2.6754 1.7696 -1.6133
H -4.4304 1.8270 0.9062
H -2.9813 -0.1801 1.8271
H -4.9979 1.7403 -0.7572
H -2.9163 3.1356 -0.5311
H -5.0017 -0.5221 0.4293
H -4.0212 -0.5163 -1.0372
H -2.8013 -1.6228 0.8386
H -1.8583 1.8724 1.3338
C -0.3936 2.4166 -0.1339
H 0.4716 2.2116 0.4998
H -0.6342 3.4810 -0.0336
H -0.1189 2.2312 -1.1749

Cartesian Coordinates of GS-(5*R**, 6*R**)-**1-ZW-S$_{ax}$** in chloroform
37
00000001 0.000000
S 1.544576 0.099998 1.965199
C 1.836406 -0.275266 0.322438
N 0.989637 -0.784556 -0.584195
N -0.277851 -1.119333 -0.111062
C -0.467131 -2.597535 -0.031394
C 0.706207 -3.360951 0.498913
O -1.494310 -3.081052 -0.436123
N 3.066355 -0.066115 -0.310924
C 4.283027 0.442225 0.128919
C 5.328803 0.450144 -0.972450
O 4.512852 0.836932 1.260692
H 1.166250 -2.847046 1.346821
H 1.463531 -3.465883 -0.284537
H 0.357163 -4.354102 0.786837
H 6.244490 0.899361 -0.586873
H 4.984691 1.022360 -1.841516
H 5.545387 -0.570065 -1.310093
H 3.047649 -0.357072 -1.287870
C -1.258096 -0.254054 0.016697
C -1.763784 2.182493 0.527421
C -3.253917 0.385306 1.431077
C -3.211737 1.795602 0.841577
C -2.629324 -0.661347 0.482695
C -1.049250 1.180519 -0.407151
H -1.196052 2.240661 1.464224
H -2.715830 0.367671 2.387512
H -3.831054 1.841389 -0.063709
H -1.711487 3.174058 0.063356
H -4.282927 0.073924 1.639570
H -3.641246 2.514193 1.549177
H -2.617427 -1.642678 0.953387
H 0.017223 1.395899 -0.395748
H -3.259507 -0.762601 -0.412304
C -1.527035 1.292358 -1.880376
H -1.338459 2.312066 -2.231573
H -2.595325 1.088412 -1.993416
H -0.972517 0.604160 -2.525913

Cartesian Coordinates of TS-(5*R**, 6*R**)-**1- ZW-S$_{ax}$** in chloroform
37
00000001 0.000000
S 2.477423 -0.101385 -1.307318
C 1.414007 -1.358155 -1.763542
N 0.232135 -1.676013 -1.206030
N -0.079310 -0.883775 -0.056563

C	0.313932	-1.387404	1.230378
C	1.183310	-2.611399	1.258162
O	-0.071509	-0.796891	2.221746
N	1.679322	-2.271895	-2.783183
C	2.647776	-2.296651	-3.783359
C	2.478200	-3.478112	-4.718029
O	3.531786	-1.466072	-3.913587
H	2.142390	-2.424638	0.766281
H	0.696107	-3.437786	0.731463
H	1.355091	-2.878731	2.301690
H	3.318964	-3.504876	-5.412117
H	1.547977	-3.384725	-5.291054
H	2.435611	-4.421836	-4.162954
H	0.963447	-2.995359	-2.852130
C	-1.297884	-0.299932	-0.226728
C	-1.574971	2.080417	0.062480
C	-2.902226	0.544105	1.562645
C	-2.877468	1.895101	0.841946
C	-2.483138	-0.621276	0.616001
C	-1.347658	0.968679	-1.026202
H	-0.718041	2.085772	0.746989
H	-2.196789	0.547616	2.398211
H	-3.736863	1.986382	0.167175
H	-1.560629	3.037024	-0.473132
H	-3.897309	0.326175	1.963428
H	-2.977101	2.702525	1.577429
H	-2.339090	-1.542983	1.181039
H	-0.359381	1.127196	-1.467288
H	-3.302246	-0.788392	-0.099452
C	-2.407563	1.014282	-2.140892
H	-2.406341	2.001949	-2.613559
H	-3.419778	0.822239	-1.775464
H	-2.179379	0.272242	-2.912323

Cartesian Coordinates of GS-(5*R**, 6*R**)-**1- ZW-S$_{eq}$** in chloroform

37

00000001 0.000000

S	1.764619	-0.013501	2.089074
C	1.870965	-0.347033	0.414367
N	0.892937	-0.695847	-0.434328
N	-0.351539	-0.897331	0.151050
C	-0.702724	-2.353901	0.158975
C	0.396496	-3.275974	0.587126
O	-1.791742	-2.690958	-0.231427
N	3.061964	-0.271537	-0.315798
C	4.364224	0.074588	0.026442
C	5.299434	0.028104	-1.168724
O	4.738041	0.388797	1.144861
H	0.962673	-2.859924	1.423895
H	1.089017	-3.436247	-0.245513
H	-0.054404	-4.232794	0.856242
H	6.317602	0.218174	-0.827683
H	5.021921	0.791126	-1.905536
H	5.261610	-0.946547	-1.668239
H	2.922015	-0.509684	-1.297109
C	-1.206973	0.036329	0.495266
C	-3.727438	-0.040586	0.398244
C	-2.401305	1.767359	-0.765109
C	-3.727197	1.408745	-0.090634
C	-1.133152	1.504510	0.125511
C	-2.465772	-0.317684	1.246109
H	-2.288182	1.205481	-1.702247
H	-3.900536	2.083659	0.758670
H	-1.288776	2.041304	1.070897
H	-2.475399	0.346014	2.119953

H	-4.552487	1.572364	-0.793610
H	-2.382624	2.828839	-1.034086
H	-4.612487	-0.252456	1.007309
H	-3.739984	-0.738151	-0.446567
H	-2.458129	-1.341139	1.615354
C	0.099440	2.099965	-0.560988
H	0.990972	2.035949	0.064869
H	-0.101144	3.161882	-0.742682
H	0.308073	1.628077	-1.523825

Cartesian Coordinates of TS-(5*R**, 6*R**)-**1- ZW-S$_{eq}$** in chloroform

37

00000001 0.000000

S	2.562305	-0.363427	-1.102730
C	1.190834	-1.258700	-1.589614
N	-0.015450	-1.280774	-1.001505
N	-0.081362	-0.470125	0.164700
C	0.537876	-1.016898	1.384603
C	0.988958	-2.450893	1.370086
O	0.583446	-0.290231	2.351531
N	1.181162	-2.158826	-2.653894
C	2.106766	-2.420287	-3.659591
C	1.605046	-3.452625	-4.650649
O	3.200251	-1.886121	-3.750870
H	0.241210	-3.087995	0.889648
H	1.145981	-2.758033	2.405614
H	1.928591	-2.565671	0.823005
H	1.374091	-4.397866	-4.146427
H	2.376210	-3.624516	-5.402022
H	0.691038	-3.106017	-5.146433
H	0.286968	-2.640100	-2.748571
C	-1.268780	0.166053	0.308002
C	-3.651558	-0.023759	1.006497
C	-3.013737	1.726873	-0.697154
C	-3.950319	1.375087	0.463594
C	-1.518558	1.490007	-0.371157
C	-2.177303	-0.128095	1.470480
H	-3.266295	1.120996	-1.577697
H	-3.832314	2.110324	1.271692
H	-1.247481	2.154238	0.472298
H	-2.012280	0.601520	2.273549
H	-4.992670	1.439656	0.130570
H	-3.143483	2.774042	-0.991285
H	-4.292875	-0.262457	1.861659
H	-3.853346	-0.780262	0.237151
H	-1.967931	-1.116092	1.886905
C	-0.618377	1.831342	-1.557591
H	0.442236	1.703034	-1.323241
H	-0.783076	2.873849	-1.849545
H	-0.851064	1.201045	-2.422006

Cartesian Coordinates of TS-(5*R**, 6*S**)-**2-S$_{ax}$** in chloroform, imaginary frequency: - 55.819 cm^{-1}

46

M0001 0.000000

S	1.4177	0.1675	1.7496
C	1.7941	-0.1749	0.1091
N	1.0049	-0.7620	-0.7940
N	-0.1812	-1.2528	-0.2459
C	-0.3294	-2.6950	-0.3129
C	0.9344	-3.4703	-0.5479
O	-1.4316	-3.1953	-0.2215
N	3.0208	0.1306	-0.4753
C	4.0944	0.9004	-0.0390
C	5.1800	1.0234	-1.0906

O 4.1714 1.4219 1.0618
H 1.6901 -3.2224 0.2041
H 1.3611 -3.2297 -1.5258
H 0.6895 -4.5324 -0.5008
H 5.9995 1.6173 -0.6855
H 4.7957 1.5101 -1.9941
H 5.5596 0.0366 -1.3796
H 3.0829 -0.2108 -1.4344
C -1.0537 -0.4348 0.3701
C -1.6714 1.9214 1.0474
C -2.4270 -0.0017 2.4617
C -2.8055 1.3748 1.9189
C -2.0704 -0.9918 1.3351
C -1.2214 0.9961 -0.1148
H -0.7909 2.0631 1.6845
H -1.5692 0.0883 3.1389
H -3.7450 1.3114 1.3558
H -1.9220 2.9082 0.6527
H -3.2494 -0.4367 3.0400
H -2.9911 2.0674 2.7490
H -1.7202 -1.9327 1.7579
H -0.2493 1.3662 -0.4405
H -2.9812 -1.2312 0.7742
C -2.1166 1.0440 -1.4571
C -3.4057 0.1976 -1.4255
H -3.1982 -0.8762 -1.3550
H -3.9597 0.3506 -2.3592
H -4.0770 0.4762 -0.6071
C -2.5072 2.5112 -1.7326
H -1.6404 3.1823 -1.7025
H -3.2555 2.8878 -1.0281
H -2.9425 2.5884 -2.7358
C -1.2665 0.5629 -2.6548
H -0.3457 1.1473 -2.7580
H -1.8416 0.6790 -3.5815
H -0.9807 -0.4901 -2.5814

Cartesian Coordinates of TS-(5*R**, 6*S**)-**2-S$_{eq}$** in chloroform, imaginary frequency: - 33.363 cm^{-1}
46
M0001 0.000000
S 1.5148 0.2909 1.6043
C 2.0601 -0.0252 0.0130
N 1.3209 -0.1991 -1.0864
N -0.0497 -0.2975 -0.8704
C -0.6453 -1.4094 -1.5822
C 0.2516 -2.5866 -1.8377
O -1.7827 -1.3111 -1.9908
N 3.4075 -0.1499 -0.3236
C 4.5751 0.1109 0.3842
C 5.8183 -0.1256 -0.4524
O 4.6137 0.4865 1.5453
H 0.8384 -2.8495 -0.9543
H 0.9598 -2.3485 -2.6378
H -0.3721 -3.4255 -2.1516
H 6.7004 0.0233 0.1711
H 5.8560 0.5717 -1.2976
H 5.8309 -1.1430 -0.8596
H 3.5347 -0.4167 -1.2994
C -0.7310 0.6293 -0.1750
C -3.1402 1.2403 -0.5054
C -1.2700 2.7540 -1.3023
C -2.7125 2.6826 -0.8027
C -0.2943 2.0681 -0.3051
C -2.1262 0.5059 0.4339
H -1.1805 2.2722 -2.2849

H -2.8087 3.2880 0.1095
H -0.3485 2.5674 0.6645
H -2.0013 1.1947 1.2806
H -3.3923 3.1214 -1.5430
H 0.7285 2.1452 -0.6682
H -0.9446 3.7931 -1.4268
H -4.1162 1.2445 -0.0105
H -3.2471 0.6692 -1.4320
C -2.7172 -0.8120 1.1038
C -3.8104 -1.5263 0.2757
H -3.4530 -1.8593 -0.6991
H -4.6898 -0.8942 0.1160
H -4.1528 -2.4104 0.8276
C -1.6421 -1.8478 1.4861
H -0.7872 -1.3967 1.9978
H -1.2622 -2.4006 0.6209
H -2.0792 -2.5963 2.1582
C -3.3806 -0.3315 2.4176
H -2.6375 0.0623 3.1219
H -3.9014 -1.1595 2.9124
H -4.1222 0.4550 2.2335

Cartesian Coordinates of GS-(5*R**, 6*S**)-**2- ZW-S$_{ax}$** in chloroform
46
00000001 0.000000
S 2.177419 -0.966481 1.904982
C 2.298845 -0.491689 0.268115
N 1.422174 -0.677247 -0.730698
N 0.274072 -1.398296 -0.408183
C 0.294095 -2.750863 -1.041916
C 1.577881 -3.506507 -0.892894
O -0.669769 -3.112221 -1.669051
N 3.402543 0.192005 -0.256002
C 4.528394 0.757461 0.331737
C 5.422831 1.439335 -0.688226
O 4.790288 0.725636 1.523253
H 2.011768 -3.363782 0.099961
H 2.301442 -3.151490 -1.634143
H 1.372997 -4.561362 -1.084288
H 6.289027 1.857391 -0.174425
H 4.887853 2.245949 -1.202940
H 5.764608 0.728425 -1.449361
H 3.314328 0.346916 -1.259809
C -0.796881 -0.882516 0.153213
C -1.377200 0.836742 1.907120
C -2.276364 -1.524175 2.046296
C -2.549629 -0.051390 2.348999
C -1.961161 -1.744164 0.545655
C -0.860229 0.594963 0.460387
H -0.529411 0.655453 2.577964
H -1.432467 -1.887135 2.645841
H -3.479137 0.251437 1.856052
H -1.636991 1.894640 2.018116
H -3.142911 -2.143888 2.300609
H -2.710758 0.083953 3.425298
H -1.783366 -2.798237 0.344969
H 0.162847 0.965236 0.419145
H -2.832769 -1.446539 -0.049844
C -1.621897 1.413958 -0.690128
C -3.151597 1.478033 -0.528470
H -3.633606 0.495984 -0.570406
H -3.572610 2.069387 -1.350511
H -3.448702 1.968155 0.403690
C -1.072223 2.854946 -0.624968
H 0.001962 2.883204 -0.841052

H	-1.228145	3.312230	0.358193
H	-1.577156	3.488085	-1.363846
C	-1.294780	0.835099	-2.083085
H	-0.215247	0.756553	-2.248730
H	-1.708696	1.485785	-2.862536
H	-1.731422	-0.159928	-2.232663

Cartesian Coordinates of TS-(5*R**, 6*S**)-**2- ZW-S$_{ax}$** in chloroform

46

00000001 0.000000

S	2.973538	0.358259	-0.958274
C	1.906271	-0.450677	-2.023605
N	0.762745	-1.072586	-1.703218
N	0.514563	-1.071918	-0.301009
C	1.173077	-2.131559	0.459385
C	1.943522	-3.166650	-0.309917
O	1.044102	-2.129800	1.664729
N	2.136826	-0.612140	-3.389157
C	3.080915	-0.049907	-4.243245
C	2.893623	-0.491092	-5.681517
O	3.962561	0.717085	-3.891649
H	2.833817	-2.734440	-0.774606
H	1.324562	-3.590007	-1.106427
H	2.248158	-3.945653	0.390810
H	3.703608	-0.080636	-6.285196
H	1.935995	-0.131311	-6.075855
H	2.898711	-1.583719	-5.762304
H	1.423362	-1.183512	-3.841786
C	-0.755088	-0.710387	0.016638
C	-1.142122	1.066922	1.629753
C	-1.913293	-1.273122	2.229263
C	-2.159123	0.226048	2.409036
C	-1.674673	-1.641405	0.738887
C	-1.037822	0.775274	0.088323
H	-0.143175	0.906987	2.052410
H	-1.022172	-1.581718	2.781926
H	-3.180588	0.478223	2.114714
H	-1.353364	2.136655	1.734875
H	-2.759167	-1.858116	2.604870
H	-2.076720	0.480166	3.473503
H	-1.339880	-2.676816	0.649925
H	-0.113035	1.255783	-0.246484
H	-2.632620	-1.566380	0.203005
C	-2.165155	1.393426	-0.838201
C	-3.619797	1.192736	-0.370924
H	-3.889708	0.140815	-0.233032
H	-4.298441	1.594049	-1.133430
H	-3.836649	1.727279	0.558839
C	-1.903253	2.911521	-0.938055
H	-0.907232	3.119931	-1.346504
H	-1.979455	3.416589	0.031670
H	-2.638075	3.381024	-1.602470
C	-2.019161	0.789869	-2.250370
H	-1.000899	0.898483	-2.636013
H	-2.703513	1.287004	-2.948667
H	-2.257308	-0.280821	-2.262249

Cartesian Coordinates of GS-(5*R**, 6*S**)-**2- ZW-S$_{eq}$** in chloroform

46

00000001 0.000000

S	2.395411	-1.937537	1.544039
C	1.952038	-1.246490	0.045663
N	0.729206	-0.901489	-0.364716
N	-0.321513	-1.286647	0.448448
C	-0.390918	-2.757163	0.839076

C	-0.028098	-3.700958	-0.277201
O	-0.855881	-3.072229	1.901229
N	2.861129	-0.971014	-0.980255
C	4.248721	-0.867952	-0.989428
C	4.792346	-0.534322	-2.365381
O	4.963181	-1.022955	-0.012063
H	1.023060	-3.992959	-0.200250
H	-0.191516	-3.250761	-1.258414
H	-0.641745	-4.597024	-0.157524
H	5.879928	-0.477741	-2.311651
H	4.400753	0.426007	-2.720261
H	4.506595	-1.300895	-3.094770
H	2.400709	-0.718418	-1.853806
C	-1.353324	-0.488446	0.623088
C	-3.498988	-1.040179	-0.433386
C	-2.097446	0.953506	-1.198889
C	-3.501725	0.333050	-1.116706
C	-1.435986	0.977091	0.216130
C	-2.725684	-1.038390	0.923264
H	-1.457631	0.397673	-1.894656
H	-4.156373	1.014381	-0.556764
H	-2.225263	1.343948	0.883115
H	-3.228975	-0.377483	1.634795
H	-3.931425	0.242724	-2.121511
H	-2.165696	1.978376	-1.576895
H	-4.521713	-1.382399	-0.241140
H	-3.033446	-1.785666	-1.091044
H	-2.717017	-2.036086	1.351466
C	-0.283766	2.033498	0.420518
C	0.664839	2.210211	-0.780044
H	1.397658	2.994679	-0.553984
H	0.120926	2.529516	-1.676378
H	1.206471	1.296094	-1.018429
C	-0.995638	3.392386	0.641341
H	-0.256393	4.192681	0.761493
H	-1.618007	3.381013	1.544490
H	-1.636424	3.667829	-0.204059
C	0.511260	1.721721	1.702824
H	1.205886	2.541043	1.926246
H	1.102572	0.804917	1.631481
H	-0.154721	1.622650	2.569975

Cartesian Coordinates of TS-(5*R**, 6*S**)-**2- ZW-S$_{eq}$** in chloroform

46

00000001 0.000000

S	2.322780	-1.809408	-1.019974
C	0.699531	-2.246757	-1.033596
N	-0.187549	-2.156957	0.025439
N	0.117072	-1.205048	1.019966
C	0.367026	-1.618281	2.350296
C	1.216782	-2.850376	2.492682
O	-0.061882	-0.951403	3.278821
N	0.062977	-2.916082	-2.066064
C	0.506580	-3.353465	-3.319750
C	-0.564419	-4.116181	-4.071736
O	1.620734	-3.144225	-3.765300
H	2.166961	-2.728565	1.963417
H	0.707984	-3.710420	2.042118
H	1.392218	-3.040502	3.552327
H	-0.175641	-4.400677	-5.049776
H	-1.463595	-3.504230	-4.206638
H	-0.853941	-5.020117	-3.523228
H	-0.895846	-3.176498	-1.836348
C	-1.140670	-0.643493	0.668381
C	-3.217847	-1.492028	-0.532260

C	-1.987010	0.577146	-1.323693
C	-3.342672	-0.128586	-1.215426
C	-1.307436	0.734699	0.076931
C	-2.444788	-1.410988	0.799754
H	-1.315902	0.015900	-1.984598
H	-4.037425	0.507841	-0.650821
H	-2.106164	1.127275	0.730487
H	-3.068822	-0.867122	1.526564
H	-3.776889	-0.251196	-2.215071
H	-2.115286	1.567859	-1.767348
H	-4.207099	-1.918686	-0.333670
H	-2.695350	-2.191979	-1.193535
H	-2.263320	-2.404780	1.209369
C	-0.177529	1.822476	0.135516
C	0.814288	1.720211	-1.037626
H	1.589592	2.491027	-0.941675
H	0.328568	1.876885	-2.007309
H	1.321697	0.751568	-1.061119
C	-0.880550	3.200566	0.071406
H	-0.133813	4.003057	0.068114
H	-1.528075	3.360431	0.942266
H	-1.491265	3.325419	-0.828766
C	0.605265	1.775489	1.464389
H	1.193335	2.694609	1.577219
H	1.300947	0.934795	1.502600
H	-0.059022	1.701558	2.332909

Cartesian Coordinates of TS-(5*R**, 7*S**)-**3-S$_{ax}$** in chloroform, imaginary frequency: - 70.896 cm^{-1}

37

M0001	0.000000		
S	0.7063	0.9370	1.1115
C	1.4875	-0.0870	-0.0246
N	0.9207	-1.0389	-0.7682
N	-0.4055	-1.2961	-0.4133
C	-0.6489	-2.6379	0.0809
C	0.5764	-3.4380	0.4197
O	-1.7806	-3.0687	0.1638
N	2.8503	-0.0261	-0.3029
C	3.8407	0.8725	0.0775
C	5.1818	0.5532	-0.5547
O	3.6692	1.8132	0.8368
H	1.1914	-2.9212	1.1628
H	1.2005	-3.5900	-0.4653
H	0.2438	-4.4002	0.8118
H	5.9173	1.2818	-0.2118
H	5.1186	0.5924	-1.6486
H	5.5157	-0.4533	-0.2758
H	3.1400	-0.7497	-0.9607
C	-1.3303	-0.3223	-0.4823
C	-1.9521	2.0387	-1.2650
C	-3.4750	0.8277	0.3793
C	-3.3978	1.7654	-0.8388
C	-2.6960	-0.4894	0.1242
C	-1.1941	0.7350	-1.5472
H	-3.9429	1.3131	-1.6790
H	-4.5220	0.5231	0.5024
H	-3.9078	2.7095	-0.6114
H	-2.6476	-1.0854	1.0358
H	-0.1540	0.9136	-1.8094
H	-3.2660	-1.1004	-0.5915
H	-1.6605	0.2511	-2.4255
H	-1.9340	2.6484	-2.1749
H	-1.4186	2.6066	-0.4952
C	-3.0553	1.5120	1.6880

H -2.0107 1.8377 1.6737
H -3.1706 0.8325 2.5412
H -3.6824 2.3905 1.8825

Cartesian Coordinates of TS-(5*R**, 7*S**)-**3-S$_{eq}$** in chloroform, imaginary frequency: - 43.623 cm^{-1}
37
M0001 0.000000
S 1.3263 0.6775 1.6028
C 1.7171 0.0028 0.0765
N 0.8932 -0.6066 -0.7868
N -0.3923 -0.8102 -0.2930
C -0.7716 -2.2135 -0.1522
C 0.3637 -3.1933 -0.1903
O -1.9403 -2.5204 -0.0621
N 3.0038 0.0046 -0.4613
C 4.2075 0.5510 -0.0298
C 5.3411 0.2748 -1.0004
O 4.3584 1.1769 1.0073
H 1.1064 -2.9662 0.5812
H 0.8773 -3.1442 -1.1548
H -0.0493 -4.1909 -0.0352
H 6.2568 0.7231 -0.6137
H 5.1243 0.6955 -1.9890
H 5.4944 -0.8037 -1.1239
H 3.0403 -0.4807 -1.3573
C -1.1683 0.2185 0.0573
C -3.6905 0.3218 -0.0325
C -2.2294 1.7642 -1.5396
C -3.5566 1.6569 -0.7828
C -1.0002 1.5511 -0.6081
C -2.4308 0.0861 0.8541
H -3.6340 2.4838 -0.0620
H -0.9812 2.3355 0.1534
H -2.3855 0.8907 1.6003
H -4.3935 1.7726 -1.4828
H -3.7283 -0.4956 -0.7650
H -2.5043 -0.8625 1.3801
H -0.0731 1.6042 -1.1763
H -2.1978 1.0300 -2.3554
H -2.1241 2.7516 -2.0027
C -4.9584 0.2630 0.8239
H -5.0533 -0.7000 1.3385
H -5.8528 0.3971 0.2042
H -4.9623 1.0527 1.5861

Cartesian Coordinates of **TS-TsC-S$_{ax}$** in chloroform, imaginary frequency: - 53.438 cm^{-1}
34
M0001 0.000000
S 0.7073 0.8068 1.3420
C 1.2903 -0.0942 0.0056
N 0.5969 -0.8981 -0.8113
N -0.7225 -1.1002 -0.4109
C -1.0265 -2.4745 -0.0044
C 0.1550 -3.3029 0.4028
O -2.1668 -2.8774 -0.0542
N 2.6258 -0.0911 -0.3968
C 3.7305 0.6470 0.0138
C 4.9739 0.3130 -0.7894
O 3.7238 1.4749 0.9108
H 0.7460 -2.7952 1.1709
H 0.8147 -3.4764 -0.4524
H -0.2195 -4.2554 0.7801
H 5.8250 0.8427 -0.3597
H 4.8524 0.6213 -1.8349

H 5.1762 -0.7643 -0.7807
H 2.7911 -0.7294 -1.1747
C -1.6110 -0.1099 -0.4007
C -1.9671 2.4071 -0.7545
C -3.4385 1.1184 0.8318
C -3.3853 2.2485 -0.1982
C -2.9568 -0.2314 0.2552
C -1.4172 1.0789 -1.3006
H -4.0873 2.0357 -1.0168
H -4.4605 0.9756 1.1991
H -3.7151 3.1893 0.2581
H -2.9586 -1.0010 1.0253
H -0.3852 1.1684 -1.6323
H -3.6643 -0.5677 -0.5168
H -2.0138 0.8039 -2.1896
H -1.9481 3.1449 -1.5642
H -2.8195 1.3750 1.7005
H -1.2927 2.7710 0.0284

Cartesian Coordinates of **TS-TsC-**S_{eq} in chloroform, imaginary frequency: - 39.057 cm^{-1}
34
M0001 0.000000
S 1.0978 0.6209 1.6089
C 1.4165 -0.0328 0.0556
N 0.5449 -0.6080 -0.7829
N -0.7243 -0.7817 -0.2387
C -1.1468 -2.1730 -0.1126
C -0.0411 -3.1864 -0.1111
O -2.3268 -2.4423 -0.0517
N 2.6798 -0.0406 -0.5322
C 3.9016 0.4967 -0.1407
C 4.9912 0.2488 -1.1666
O 4.0955 1.0953 0.9054
H 0.6844 -2.9666 0.6789
H 0.5002 -3.1683 -1.0611
H -0.4865 -4.1693 0.0481
H 5.9185 0.7026 -0.8158
H 4.7227 0.6810 -2.1373
H 5.1506 -0.8259 -1.3130
H 2.6751 -0.5061 -1.4395
C -1.4343 0.2613 0.2022
C -3.9346 0.4183 0.1960
C -2.5197 1.8713 -1.3186
C -3.8229 1.7702 -0.5192
C -1.2666 1.6126 -0.4288
C -2.6673 0.1272 1.0448
H -3.8623 2.5831 0.2192
H -1.2167 2.3733 0.3545
H -2.5798 0.9007 1.8183
H -4.6816 1.9116 -1.1864
H -4.0594 -0.3930 -0.5301
H -2.7406 -0.8396 1.5376
H -0.3560 1.6727 -1.0222
H -2.5268 1.1514 -2.1473
H -2.4084 2.8659 -1.7646
H -4.8062 0.3948 0.8591

Cartesian Coordinates of **GS-TsC-ZW-**S_{ax} in chloroform
4
M0001 0.000000
S 1.196365 0.316715 1.681146
C 1.602544 -0.138321 0.083118
N 0.829181 -0.721632 -0.844858
N -0.449132 -1.062593 -0.412715
C -0.652361 -2.527234 -0.294853

C	0.548019	-3.303735	0.148887
O	-1.720477	-3.000154	-0.597832
N	2.866343	0.070915	-0.476833
C	4.044662	0.611240	0.025316
C	5.154648	0.621490	-1.010798
O	4.196846	1.032178	1.160846
H	1.023457	-2.831458	1.013502
H	1.288664	-3.345884	-0.655616
H	0.221896	-4.315813	0.392808
H	6.049737	1.056775	-0.565175
H	4.866611	1.210954	-1.888787
H	5.382001	-0.395211	-1.351965
H	2.916133	-0.258301	-1.440619
C	-1.413399	-0.181681	-0.238563
C	-1.840626	2.307788	0.177073
C	-3.221514	0.553050	1.337329
C	-3.234955	1.940771	0.693776
C	-2.747292	-0.541220	0.351958
C	-1.268868	1.220172	-0.753586
H	-1.150908	2.449194	1.017098
H	-2.560734	0.553672	2.213244
H	-3.957159	1.953510	-0.134564
H	-1.866745	3.251451	-0.378174
H	-4.220554	0.273530	1.688129
H	-3.574442	2.689990	1.418536
H	-2.727771	-1.513920	0.839151
H	-0.242263	1.433726	-1.043207
H	-3.466912	-0.619798	-0.474872
H	-1.870995	1.209837	-1.678899

Cartesian Coordinates of **TS-TsC-ZW-S$_{ax}$** in chloroform

34

M0001 0.000000

S	2.708834	0.660274	-0.618583
C	1.642744	-0.592487	-1.080081
N	0.463610	-0.913739	-0.520036
N	0.151758	-0.126113	0.632454
C	0.534447	-0.637099	1.919010
C	1.414682	-1.853148	1.946004
O	0.137538	-0.054808	2.910801
N	1.898084	-1.495626	-2.111669
C	2.866638	-1.517961	-3.111642
C	2.680748	-2.680802	-4.066531
O	3.764570	-0.699923	-3.225231
H	2.383943	-1.643359	1.484033
H	0.953474	-2.674156	1.388655
H	1.562470	-2.139330	2.988182
H	3.523568	-2.709951	-4.757913
H	1.754414	-2.562790	-4.641207
H	2.620555	-3.632391	-3.526837
H	1.173761	-2.209576	-2.190881
C	-1.063504	0.463689	0.459209
C	-1.339994	2.866674	0.721468
C	-2.680573	1.334354	2.219112
C	-2.653697	2.674692	1.479411
C	-2.259800	0.155530	1.290337
C	-1.117563	1.727698	-0.326978
H	-0.488307	2.894872	1.411671
H	-1.980706	1.349221	3.059420
H	-3.493219	2.736441	0.774140
H	-1.333050	3.808513	0.162182
H	-3.678259	1.122219	2.616514
H	-2.788588	3.491769	2.198597
H	-2.134657	-0.763372	1.864094
H	-0.191462	1.884183	-0.883486

H	-3.068650	-0.002882	0.560142
H	-1.963809	1.739384	-1.024359

Cartesian Coordinates of **GS-TsC-ZW**-S_{eq} in chloroform

34

M0001 0.000000

S	1.705246	0.306871	2.003819
C	1.823405	-0.119909	0.353458
N	0.872552	-0.611740	-0.457161
N	-0.362865	-0.847467	0.133593
C	-0.693950	-2.296302	0.191479
C	0.452343	-3.190495	0.547627
O	-1.812064	-2.655970	-0.083209
N	2.998079	0.003060	-0.395853
C	4.277353	0.450555	-0.087107
C	5.203554	0.403219	-1.289249
O	4.638556	0.846357	1.009495
H	1.043081	-2.766058	1.364323
H	1.114735	-3.310006	-0.315704
H	0.047932	-4.165458	0.824263
H	6.209443	0.678788	-0.970797
H	4.869440	1.105506	-2.062172
H	5.227625	-0.597118	-1.736194
H	2.867637	-0.304064	-1.359256
C	-1.199916	0.099702	0.494707
C	-3.679288	0.269348	0.256047
C	-2.139590	1.965279	-0.829198
C	-3.515024	1.724969	-0.197469
C	-0.975602	1.527006	0.106645
C	-2.509124	-0.161237	1.177910
H	-2.057715	1.418582	-1.777527
H	-3.642089	2.391619	0.666612
H	-0.990349	2.136681	1.015915
H	-2.508542	0.483148	2.066622
H	-4.303745	1.985921	-0.912854
H	-1.996236	3.025539	-1.063646
H	-4.617780	0.132950	0.803550
H	-3.709414	-0.405250	-0.607639
H	-2.626325	-1.190928	1.506789
H	-0.011360	1.666901	-0.377819

Cartesian Coordinates of **TS-TsC-ZW**-S_{eq} in chloroform

34

M0001 0.000000

S	3.131423	-0.146332	-0.498238
C	1.734477	-0.729606	-1.297203
N	0.491086	-0.730633	-0.811909
N	0.449881	-0.263812	0.519048
C	1.029781	-1.241182	1.516024
C	1.533169	-0.628751	2.795069
O	1.051708	-2.415956	1.254052
N	1.741343	-1.320139	-2.559040
C	2.735837	-1.422750	-3.526142
C	2.243724	-2.094492	-4.793095
O	3.876955	-1.011761	-3.390406
H	1.613008	0.457369	2.740797
H	2.522905	-1.048100	2.993466
H	0.881220	-0.917260	3.626131
H	3.093664	-2.269750	-5.453540
H	1.519795	-1.453004	-5.309562
H	1.749683	-3.047707	-4.574735
H	0.821537	-1.658247	-2.839636
C	-0.618820	0.453166	0.865987
C	-2.909608	0.521898	1.835120
C	-2.199814	2.350203	0.229749

C	-3.038802	2.004454	1.467476
C	-0.744401	1.873353	0.388059
C	-1.429978	0.125991	2.087174
H	-2.632514	1.873650	-0.659605
H	-2.709079	2.618209	2.317556
H	-0.258148	2.441029	1.197959
H	-1.066364	0.707145	2.946644
H	-4.091097	2.255329	1.289954
H	-2.209542	3.429806	0.045393
H	-3.479946	0.293441	2.741522
H	-3.323089	-0.103986	1.034033
H	-1.355169	-0.934932	2.340234
H	-0.154825	2.033355	-0.518338

Cartesian Coordinates of GS-(5*R**, 6*S**)-**2-ZW-S$_{eq}$** in ethyl acetate

46

00000001 0.000000

S	2.411465	-2.101914	1.402890
C	1.968590	-1.274772	-0.025948
N	0.745372	-0.878569	-0.376624
N	-0.288428	-1.274888	0.448286
C	-0.314443	-2.721005	0.967765
C	-0.076360	-3.750349	-0.102145
O	-0.774787	-2.939760	2.058826
N	2.865862	-0.936700	-1.039973
C	4.256059	-0.889823	-1.070732
C	4.785042	-0.436620	-2.417470
O	4.980912	-1.173604	-0.129692
H	0.429239	-4.614778	0.330365
H	0.484476	-3.368493	-0.953377
H	-1.064540	-4.077570	-0.453640
H	5.874318	-0.405257	-2.379814
H	4.405880	0.559317	-2.673221
H	4.472318	-1.125687	-3.210577
H	2.399864	-0.593351	-1.880404
C	-1.334446	-0.491049	0.605859
C	-3.460033	-1.063049	-0.475187
C	-2.085789	0.956376	-1.219308
C	-3.481246	0.315596	-1.147211
C	-1.434235	0.972675	0.198273
C	-2.699973	-1.064308	0.889711
H	-1.435852	0.413978	-1.916485
H	-4.147816	0.983014	-0.584419
H	-2.231929	1.326962	0.862933
H	-3.223594	-0.423469	1.605305
H	-3.906469	0.226253	-2.154075
H	-2.166712	1.983548	-1.589041
H	-4.478507	-1.424715	-0.295839
H	-2.975537	-1.792685	-1.137027
H	-2.677700	-2.068898	1.302908
C	-0.291663	2.035293	0.423787
C	0.664219	2.233446	-0.766921
H	1.383087	3.028515	-0.531810
H	0.123357	2.548158	-1.666676
H	1.222581	1.329278	-1.004108
C	-1.013464	3.386417	0.656368
H	-0.281214	4.190987	0.792176
H	-1.643155	3.360090	1.554207
H	-1.649740	3.667377	-0.190729
C	0.496778	1.712862	1.707695
H	1.195267	2.526739	1.939464
H	1.083016	0.792611	1.632838
H	-0.172692	1.611610	2.571870

Cartesian Coordinates of TS-(5*R**, 6*S**)-**2-ZW-S$_{eq}$** in ethyl acetate

46

00000001 0.000000

S	2.334664	-1.823275	-0.992283
C	0.705962	-2.242032	-1.018407
N	-0.179785	-2.152165	0.043030
N	0.125663	-1.199505	1.035643
C	0.376497	-1.613246	2.366020
C	1.210320	-2.856823	2.504402
O	-0.039778	-0.941864	3.296981
N	0.060748	-2.881607	-2.061569
C	0.503873	-3.329574	-3.312040
C	-0.586384	-4.050125	-4.077071
O	1.631054	-3.160852	-3.743673
H	2.150742	-2.758589	1.953293
H	0.676829	-3.713177	2.074990
H	1.404774	-3.039753	3.562031
H	-0.208041	-4.326702	-5.061627
H	-1.471149	-3.414835	-4.197127
H	-0.896465	-4.957007	-3.544830
H	-0.908292	-3.117906	-1.843064
C	-1.135952	-0.648143	0.677680
C	-3.207033	-1.512565	-0.525650
C	-1.980140	0.552538	-1.328854
C	-3.334650	-0.154533	-1.218143
C	-1.306412	0.724422	0.072540
C	-2.438294	-1.420986	0.807398
H	-1.306550	-0.015479	-1.981763
H	-4.031428	0.484232	-0.658753
H	-2.108275	1.121704	0.719275
H	-3.068451	-0.877322	1.529035
H	-3.767104	-0.284607	-2.217572
H	-2.107820	1.538450	-1.783434
H	-4.195320	-1.941219	-0.326674
H	-2.681688	-2.215793	-1.181050
H	-2.253827	-2.412150	1.222130
C	-0.179004	1.814705	0.125482
C	0.820469	1.701729	-1.040004
H	1.589946	2.479750	-0.951776
H	0.340041	1.840340	-2.015191
H	1.335685	0.736978	-1.046192
C	-0.883091	3.190801	0.043149
H	-0.137954	3.994888	0.033766
H	-1.534630	3.359593	0.909484
H	-1.490767	3.304854	-0.860593
C	0.597528	1.782805	1.458239
H	1.184875	2.703522	1.564480
H	1.293460	0.942925	1.509132
H	-0.070319	1.718359	2.324802

Cartesian Coordinates of GS-(5*R**, 6*S**)-**2-ZW-S$_{eq}$** in 2-propanol

46

00000001 0.000000

S	2.423758	-1.933515	1.578028
C	1.963196	-1.247050	0.070775
N	0.746086	-0.904862	-0.339713
N	-0.317444	-1.288746	0.462677
C	-0.402282	-2.762581	0.813460
C	-0.050672	-3.683645	-0.320375
O	-0.837638	-3.099449	1.884473
N	2.873239	-0.980133	-0.957174
C	4.255394	-0.870479	-0.979837
C	4.788378	-0.541439	-2.355713
O	4.981269	-1.017814	-0.000512
H	1.002142	-3.975586	-0.255301

H	-0.220085	-3.218589	-1.292950
H	-0.660575	-4.583595	-0.210935
H	5.877027	-0.495898	-2.316319
H	4.402090	0.424091	-2.702792
H	4.484585	-1.301772	-3.084019
H	2.409616	-0.733675	-1.832286
C	-1.350315	-0.487980	0.629640
C	-3.497510	-1.044868	-0.422851
C	-2.095470	0.943120	-1.195659
C	-3.499871	0.325437	-1.109953
C	-1.433158	0.975478	0.220954
C	-2.720331	-1.038009	0.932671
H	-1.455921	0.384306	-1.888913
H	-4.153428	1.009742	-0.552682
H	-2.223721	1.342715	0.885392
H	-3.221739	-0.373583	1.641895
H	-3.929018	0.231694	-2.114569
H	-2.161506	1.966865	-1.576398
H	-4.519320	-1.384436	-0.222563
H	-3.036637	-1.794832	-1.078120
H	-2.710866	-2.033946	1.365103
C	-0.285049	2.036836	0.417422
C	0.660930	2.207585	-0.785282
H	1.397905	2.989692	-0.563885
H	0.116138	2.526942	-1.680665
H	1.199130	1.291266	-1.023571
C	-1.002116	3.393711	0.630023
H	-0.266580	4.198837	0.741788
H	-1.621791	3.387187	1.535039
H	-1.646446	3.659891	-0.215275
C	0.512704	1.739035	1.701057
H	1.198230	2.566727	1.922382
H	1.116160	0.829369	1.635307
H	-0.151109	1.635743	2.569302

Cartesian Coordinates of TS-(5*R**, 6*S**)-**2-ZW-S**$_{eq}$ in 2-propanol

46

00000001 0.000000

S	2.347483	-1.788250	-1.030403
C	0.724974	-2.279944	-1.058058
N	-0.186722	-2.183003	-0.043513
N	0.070476	-1.224265	0.959761
C	0.339012	-1.621860	2.283131
C	1.172844	-2.861587	2.434980
O	-0.074743	-0.940508	3.215702
N	0.142206	-3.000187	-2.090855
C	0.632190	-3.485600	-3.301790
C	-0.402078	-4.276633	-4.066934
O	1.772014	-3.296142	-3.709962
H	2.122869	-2.762151	1.900992
H	0.649061	-3.720494	1.999646
H	1.349732	-3.040556	3.496322
H	0.017600	-4.581410	-5.025953
H	-1.304640	-3.680380	-4.242101
H	-0.696663	-5.169879	-3.503813
H	-0.824802	-3.259406	-1.889535
C	-1.177980	-0.617595	0.643884
C	-3.285427	-1.420778	-0.527793
C	-2.085210	0.681779	-1.266608
C	-3.435052	-0.027861	-1.138235
C	-1.335847	0.776611	0.111940
C	-2.468714	-1.386357	0.782968
H	-1.442403	0.158625	-1.983524
H	-4.108396	0.580758	-0.520216
H	-2.102178	1.158828	0.809788

H	-3.065062	-0.857813	1.543295
H	-3.902709	-0.103097	-2.127248
H	-2.229202	1.695226	-1.648571
H	-4.264650	-1.860917	-0.312822
H	-2.777320	-2.088061	-1.232493
H	-2.275519	-2.391391	1.156768
C	-0.183646	1.841330	0.145805
C	0.739191	1.753139	-1.083153
H	1.540446	2.499507	-1.006043
H	0.205190	1.957047	-2.017543
H	1.219745	0.773439	-1.168616
C	-0.859034	3.234242	0.157898
H	-0.095463	4.020730	0.142540
H	-1.459926	3.380925	1.063698
H	-1.508409	3.400608	-0.707355
C	0.666995	1.743974	1.428362
H	1.291036	2.641120	1.524582
H	1.335830	0.880925	1.417019
H	0.047424	1.678066	2.329693